All-Optical Double Spectral-Efficient RoF Link With Compensation of Dispersion-Induced Power Fading

Dongjuan Shan, Aijun Wen, *Senior Member, IEEE*, Weile Zhai, and Meng Tan

***Abstract*—An all-optical radio-over-fiber (RoF) link with double spectral-efficient transmission and compensation of chromatic dispersion-induced power fading is proposed and experimentally demonstrated. At the central office, a commercial dual-polarization quadrature phase-shift keying modulator is utilized to produce a polarization-multiplexed signal composed of two modulated microwave vector signals and an unmodulated optical carrier. At the remote node, by adjusting the polarization controller to introduce a proper phase shift to the unmodulated optical carrier, the two vector signals can be demodulated respectively and dispersion-induced power fading can be compensated simultaneously. The link performance is evaluated by error vector magnitude and bit error rate.**

***Index Terms*—Chromatic dispersion, double spectral efficiency, microwave photonics, radio-over-fiber link.**

I. Introduction

RADIO-OVER-FIBER (RoF) link is one research hotspot of microwave photonic link (MPL), which can take full advantage of wireless and optical worlds [1], [2]. Nowadays, RoF links with higher spectral efficiency are needed to make full utilization of finite frequency spectrum resources. Therefore, it is significant to transmit high spectral-efficient microwave vector signals such as quadrature amplitude modulation (QAM) and phase-shift keying (PSK) signals on a single fiber [3].

Numerous methods of transmitting vector signals have been proposed. In [4], a 16-QAM signal is used to directly modulate a laser diode (LD). In [5], an 8-QAM signal is single sideband modulated by a dual-electrode Mach–Zehnder modulator (MZM). To transmit multiple vector signals, optical frequency comb [6] or multiple LDs [7] are used to carry multiple vector signals. However, a light wavelength can only carry one signal, which restricts the spectral efficiency of the link. Besides, these measures are comparatively complicated and costly because of using multiple modulators and optical sources. To simplify RoF links and improve spectral efficiency, in [8], two vector signals are imposed on a carrier via an MZM and a phase modulator (PM). In [9], an MPL adopts optical independent sideband modulation, which can carry four vector signals by a light wavelength. In [10], a phase-modulated vector signal and an intensity-modulated vector signal are transmitted over a carrier by a polarization division multiplexing MZM (PDM-MZM). However, at the receiver of these links, an extra laser and a coherent detection structure are used to recover the modulated signals, which greatly increase the complexity and cost of the links. Moreover, these links using two free-running laser sources, narrow line-width laser sources and complex digital signal processing (DSP) algorithms are needed to reduce large phase noises [11]. To solve this problem, in [12], a self-homodyne-detected MPL is proposed, where a phase-modulated signal and an intensity-modulated signal are polarization multiplexed by a PDM-MZM and then two signals are recovered via a self-homodyne scheme and a DSP unit. However, this link uses a 180^{o} electric coupler and a DSP unit, so it cannot transmit high-frequency signals. [13] proposed a simple method to transmit two vector signals on an optical carrier, where two signals are respectively amplitude and phase modulated by a dual-parallel MZM (DPMZM). However, the phase-modulated signal needs to be converted into intensity-modulated signal by an optical Hilbert transformer (OHT) and then recovered by a PD. The magnitude response of the OHT is a band-stop filter. To implement OHT, the notch center must be located between the optical carrier and the +1st-order radio frequency (RF) sideband, which results in the poor performance of the system for transmitting low-frequency signals. In RoF link, when transmitted signal is a high-frequency signal, the dispersion-induced power periodic fading will severely deteriorate signal to noise ratio (SNR) and limit transmission distance [14]. However, these links in [8]–[13] cannot overcome dispersion-induced power periodic fading. To solve this problem, an MPL is proposed based on a PDM-MZM in [15]. To recover two signals at the receiver, the rotation angle and the phase difference between two orthogonal polarization states introduced by PC need to be jointly optimized, so it is difficult to implement such optimization in practice. In addition, when both the angle and phase difference are optimal, signal power is not the maximum, which reduces gain and SNR of the link. Besides, the second harmonic terms cannot be eliminated, which reduces spectral purity and affects dynamic range of the link.

In this work, we propose a novel RoF link with simultaneous double spectral-efficient transmission and compensating power fading caused by fiber-dispersion. At the central office (CO),

Manuscript received May 7, 2021; revised June 11, 2021; accepted June 12, 2021. Date of publication June 23, 2021; date of current version July 6, 2021. This work was supported in part by the National Key Research and Development Program of China under Grant 2017YFB1104800, and in part by National Natural Science Foundation of China under Grants 61974177 and 61674119. *(Corresponding author: Aijun Wen.)*

The authors are with the State Key Laboratory of Integrated Services Networks, Xidian University, Xi'an 710071, China, and also with the Collaborative Innovation Center of Information Sensing and Understanding, Xidian University, Xi'an 710071, China (e-mail: djshan@stu.xidian.edu.cn; ajwen@xidian.edu.cn; wlzhai@stu.xidian.edu.cn; mtan@stu.xidian.edu.cn).

Digital Object Identifier 10.1109/JPHOT.2021.3090065

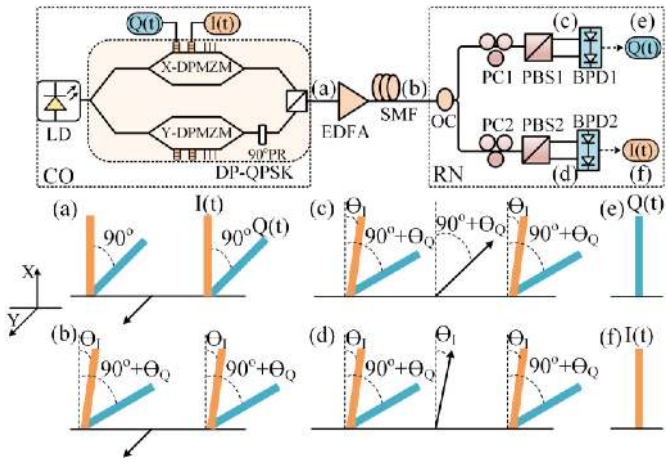

Fig. 1. The schematic of our proposed RoF link. LD, laser diode; DP-QPSK, dual-polarization quadrature phase-shift keying; EDFA, erbium-doped fiber amplifier; SMF, single-mode fiber; OC, optical coupler; PC, polarization controller; PBS, polarization beam splitter; BPD, balanced photodiode; CO, central office; RN, remote node. (a)-(f) spectral evolution diagrams at corresponding nodes.

two modulated vector signals and unmodulated optical carrier are polarization multiplexed via a commercial dual-polarization quadrature phase-shift keying (DP-QPSK) modulator. At the remote node (RN), the polarization controller (PC) is utilized to introduce a proper phase shift to unmodulated optical carrier. Subsequently, two vector signals are recovered after passing through two polarization beam splitters (PBSs) and two balanced photodiodes (BPDs) respectively. Compared with traditional RoF links, the proposed scheme can transmit two microwave vector signals over an optical carrier, so its spectral efficiency is doubled. Simultaneously, the link can also compensate the power fading caused by fiber-dispersion. The link requires only an LD, an integrated modulator and a receiver, so it is compact and simple. Besides, the proposed system is an all-optical link without filters and electrical components, so it has a wide operating frequency range. It can be applied in wireless access networks, optical fronthaul links for 5G and multiple-input multiple-output (MIMO) systems.

II. Principles

Fig. 1 shows the structure and principle of our proposed RoF link. At the CO, an optical carrier generated from an LD is sent into an integrated DP-QPSK modulator. Two vector signals I(t) and Q(t) are modulated on the optical carrier via X-DPMZM, where two sub-modulators of X-DPMZM are biased at the minimum transmission point (MITP) and main-modulator is biased at the quadrature transmission point (QTP). Y-DPMZM is not loaded with microwave signal and its three bias points all work at the maximum transmission point (MATP).

Suppose that the optical carrier output by the LD is denoted as $E_{in}(t) = E_c \cdot \exp(j\omega_c t)$, in which E_c and ω_c represent the optical amplitude and angular frequency respectively. Mathematically, two vector signals I(t) and Q(t) to be transmitted can be expressed as $I(t) = V_{\mathrm{I}}(\mathrm{t}) \sin[\omega_I t + \varphi_I(t)]$ and $Q(t) = V_Q(\mathrm{t}) \sin[\omega_Q t + \varphi_Q(t)]$, where $V_{\mathrm{I}}(\mathrm{t})$ and $V_Q(\mathrm{t})$ represent the amplitude, ω_I and ω_Q are the angular frequency, and $\varphi_{\mathrm{I}}(\mathrm{t})$ and $\varphi_Q(t)$ represent the phase of I(t) and Q(t), respectively. In the case of small signal modulation, the output field from X-DPMZM is approximately written as (1), shown at the bottom of the page, where μ represents insertion loss of the DP-QPSK modulator, $m_I(\mathrm{t}) = V_I(\mathrm{t}) \cdot \pi/(2V_\pi)$ and $m_Q(\mathrm{t}) = V_Q(\mathrm{t}) \cdot \pi/(2V_\pi)$ express the modulation depths of two vector signals, and V_π represents the half-wave voltage of X-DPMZM.

Since Y-DPMZM is not utilized to modulate RF signal and its three bias points are all biased at the MATP, its output is expressed as

$$E_Y(t) = \sqrt{\mu} E_{in}(t) \Big/ \sqrt{2} \tag{2}$$

The output signals from Y-DPMZM and X-DPMZM are polarization multiplexed. Therefore, the signal output from the DP-QPSK modulator is given by

$$E_{DPQPSK}(t) = \overrightarrow{e_X} E_X(t) + \overrightarrow{e_Y} E_Y(t) \tag{3}$$

where $\overrightarrow{e_X}$ and $\overrightarrow{e_Y}$ denote the X-polarization and Y-polarization directions. The output spectrogram of the DP-QPSK modulator is shown in Fig. 1(a). In X-polarization state, the orange spectra represent modulated I(t) and the blue spectra represent modulated Q(t), both of which are DSB-CS modes. Because the main-modulator of X-DPMZM is biased at QTP, the phase difference between modulated I(t) and Q(t) is 90°. The black spectrum represents the unmodulated optical carrier in Y-polarization state.

To compensate the insertion loss of the modulator, we use an EDFA to amplify the optical signal. The optical power input to EDFA can be indicated as

$$P_{E-in} = \frac{\mu {E_c}^2}{4} \left\{ {J_1}^2 [m_I(t)] + {J_1}^2 [m_Q(t)] + 2 \right\} \tag{4}$$

In order to avoid excessive power input to two BPDs, the EDFA is set as automatic power control mode. Assuming that its output power level is $P_{E-\mathrm{out}}$, its gain can be indicated as

$$G_E = \frac{P_{E-\mathrm{out}}}{P_{E-in}} = \frac{4P_{E-\mathrm{out}}}{\mu {E_c}^2 \left\{ {J_1}^2 [m_I(t)] + {J_1}^2 [m_Q(t)] + 2 \right\}} \tag{5}$$

Then the signal output from the EDFA is transmitted through a length of SMF. The transfer function of an SMF with length L, attenuation coefficient σ and dispersion coefficient β_2 is

$$H(j\omega) = \exp\left[-\sigma L/2 + j\beta_2 L(\omega - \omega_c)^2/2 \right] \tag{6}$$

$$E_X(t) \approx \frac{\sqrt{\mu} E_{in}(t)}{2\sqrt{2}} \left\{ \begin{array}{l} J_1 [m_I(t)] [\exp(j\omega_I t + j\varphi_I(t)) - \exp(-j\omega_I t - j\varphi_I(t))] \\ +jJ_1 [m_Q(t)] [\exp(j\omega_Q t + j\varphi_Q(t)) - \exp(-j\omega_Q t - j\varphi_Q(t))] \end{array} \right\} \tag{1}$$

After a length of SMF transmission, the modulated signals will be introduced a phase shift by fiber-dispersion. $\theta_I = L\beta_2\omega_I^2/2$ and $\theta_Q = L\beta_2\omega_Q^2/2$ express the dispersion-induced phase shifts of the $\pm$1st order sidebands of two vector signals relative to the optical carrier. The spectrogram after SMF transmission is given in Fig. 1(b). Due to the influence of fiber-dispersion, the $\pm$1st order sidebands of I(t) are introduced an extra phase shift of θ_I and $\pm$1st order sidebands of Q(t) are introduced an extra phase shift of θ_Q.

At the RN, an OC is utilized to divide the polarization-multiplexed signal to two branches. In each branch, a PC, a PBS, and a BPD compose a receiving channel. The transmission matrix of a PC combined with a PBS is [18]

$$T_{PC-PBS} = \begin{bmatrix} \cos\alpha & -\sin\alpha \cdot \exp(j\theta) \\ \sin\alpha & \cos\alpha \cdot \exp(j\theta) \end{bmatrix} \tag{7}$$

where α is the polarization azimuth between the output port of the modulator and the PBS and θ represents the phase difference between the X-polarization and Y-polarization optical signals. α and θ can be changed via the PC. Here, to maximize gain of the link, α is tuned to 45°. Therefore, the output signal of the PBS can be given by (8) and (9), shown at the bottom of the page.

The two corresponding spectrograms are represented in Fig. 1 (c) and (d), respectively. As shown in Fig. 1(c), to offset the dispersion-induced phase shift and recover Q(t), we control PC1 to adjust phase of the optical carrier as $90^o + \theta_Q$, and then we can obtain Q(t) after photoelectric conversion by BPD1. Similarly, as shown in Fig. 1(d), adjusting PC2 to introduce phase of the optical carrier as θ_I, and then we can recover I(t) after photoelectric conversion by BPD2. The carrier frequencies of two vector signals are almost same, so we have $\theta_I \approx \theta_Q$. Subsequently, the optical signal is injected into a BPD with a responsivity of η. The output two photo-currents of the upper and lower PDs in BPD are given by

$$\begin{aligned} i_u(t) &= \eta |E_{PBS-1}(t)|^2 \\ &= \frac{\eta\mu G_E E_c^2 \exp(-\sigma L)}{8} (i_{DC} + i_{SH} - i_{RF}) \end{aligned} \tag{10}$$

$$\begin{aligned} i_l(t) &= \eta |E_{PBS-2}(t)|^2 \\ &= \frac{\eta\mu G_E E_c^2 \exp(-\sigma L)}{8} (i_{DC} + i_{SH} + i_{RF}) \end{aligned} \tag{11}$$

where i_{DC} represents the direct current (DC), i_{RF} expresses the RF of interest, and i_{SH} represents the second harmonic. Their expressions are

$$i_{DC} = {J_1}^2 [m_I(t)] + {J_1}^2 [m_Q(t)] + 2 \tag{12}$$

$$\begin{aligned} i_{SH} = &-{J_1}^2 [m_I(t)] \cos[2(\omega_I t + \varphi_I(t))] \\ &- {J_1}^2 [m_Q(t)] \cos[2(\omega_Q t + \varphi_Q(t))] \end{aligned} \tag{13}$$

$$\begin{aligned} i_{RF} = &4J_1 [m_I(t)] \sin(\omega_I t + \varphi_I(t)) \sin(\theta - \theta_I) \\ &+ 4J_1 [m_Q(t)] \sin(\omega_Q t + \varphi_Q(t)) \sin(\theta - \pi/2 - \theta_Q) \end{aligned} \tag{14}$$

The i_{DC} and i_{SH} components are generated from self-beating of optical sidebands. The existence of DC term will deteriorate the noise figure of the system. The second harmonic terms reduce the spectral purity and especially for a multi-octave signal, it will limit the dynamic range of the system. The DC term can be directly blocked. However, the second harmonic terms are difficult to eliminate for a multi-octave signal, because they interfere with the fundamental signal. Fortunately, we can use BPD to remove DC and the second harmonic components. Then the output photocurrent from the BPD is given by

$$\begin{aligned} i_{BPD}(t) = i_u(t) - i_l(t) = &-\eta\mu G_E E_c^2 \exp(-\sigma L) \\ &\times \left\{ \begin{array}{c} J_1 [m_I(t)] \sin(\omega_I t + \varphi_I(t)) \sin(\theta - \theta_I) \\ +J_1 [m_Q(t)] \sin(\omega_Q t + \varphi_Q(t)) \\ \sin(\theta - \pi/2 - \theta_Q) \end{array} \right\} \end{aligned} \tag{15}$$

To compensate the dispersion-induced power fading and recover the corresponding vector signals, we control PC1 to satisfy $\theta = \theta_I$, and then we can obtain below after BPD1

$$\begin{aligned} i_{BPD1}(t) = &\eta\mu G_E E_c^2 \exp(-\sigma L) \\ &\times \{J_1 [m_Q(t)] \sin(\omega_Q t + \varphi_Q(t))\} \end{aligned} \tag{16}$$

In the same way, adjusting PC2 to meet the condition of $\theta = -\pi/2 + \theta_Q$, we have

$$\begin{aligned} i_{BPD2}(t) = &\eta\mu G_E E_c^2 \exp(-\sigma L) \\ &\times \{J_1 [m_I(t)] \sin(\omega_I t + \varphi_I(t))\} \end{aligned} \tag{17}$$

$$\begin{aligned} E_{PBS-1}(t) = &\frac{\sqrt{\mu G_E} E_{in}(t) \exp(-\sigma L/2)}{4} \\ &\times \left\{ \begin{array}{l} J_1 [m_I(t)] \exp(j\theta_I) [\exp(j\omega_I t + j\varphi_I(t)) - \exp(-j\omega_I t - j\varphi_I(t))] \\ +jJ_1 [m_Q(t)] \exp(j\theta_Q) [\exp(j\omega_Q t + j\varphi_Q(t)) - \exp(-j\omega_Q t - j\varphi_Q(t))] \\ -2\exp(j\theta) \end{array} \right\} \end{aligned} \tag{8}$$

$$\begin{aligned} E_{PBS-2}(t) = &\frac{\sqrt{\mu G_E} E_{in}(t) \exp(-\sigma L/2)}{4} \\ &\times \left\{ \begin{array}{l} J_1 [m_I(t)] \exp(j\theta_I) [\exp(j\omega_I t + j\varphi_I(t)) - \exp(-j\omega_I t - j\varphi_I(t))] \\ +jJ_1 [m_Q(t)] \exp(j\theta_Q) [\exp(j\omega_Q t + j\varphi_Q(t)) - \exp(-j\omega_Q t - j\varphi_Q(t))] \\ +2\exp(j\theta) \end{array} \right\} \end{aligned} \tag{9}$$

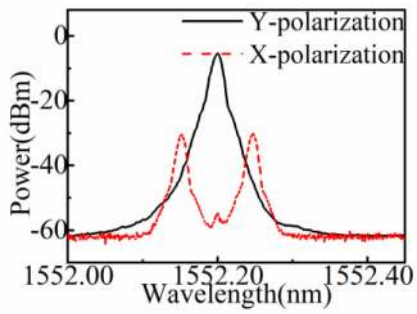

Fig. 2. The optical spectra of X-polarization and Y-polarization states output from the DP-QPSK modulator.

As can be seen from (16) and (17), by properly adjusting PC1 and PC2, the transmitted I(t) and Q(t) are recovered successfully and power fading is also eliminated. The two output electrical spectra of the two BPDs are shown in Fig. 1 (e) and (f), respectively. As shown in Fig. 1 (e) and (f), I(t) and Q(t) are recovered after SMF transmission and dispersion-induced phase shifts are also eliminated. It should be noted that in practical applications, to make the proposed link stable, the PC can be replaced by a commercial electrical polarization tracker, such as General Photonics, POS-002-E [19]. The polarization tracker can automatically control the polarization state of the system to make the system stable.

III. Experiments and Results

To verify the performance of the link, we set up an experimental link according to the structure in Fig. 1. An optical carrier with wavelength of 1552.20 nm and power of 12.5 dBm is produced by a laser source (Emcore1782) and then it is directly sent into a commercial DP-QPSK modulator (FTM7977HQA). The insertion loss of the modulator is about 9 dB and the half-wave voltage of the modulator at low frequency ($<$ 200 Hz) is about 3.2 V. Two microwave vector signals are respectively produced by two vector signal generators (R&S SMW200A and SMBV100A). Due to the limitation of the maximum output symbol rates of the two signal generators, we set I(t) as a 100-Msymbol/s QPSK signal and Q(t) as a 50-Msymbol/s 16-QAM signal in the experiment. A signal and spectrum analyzer (R&S, FSW50) is utilized to observe the demodulated signal.

Firstly, we set the carrier frequency of I(t) and Q(t) at 6 GHz. The signal output from the DP-QPSK modulator is recorded by an optical spectrum analyzer (Advantest, Q8384). As shown in Fig. 2, the spectrum of X-polarization state is a DSB-CS signal, where the suppression ratio of signal sideband to optical carrier is about 25 dB. The spectrum of Y-polarization state contains only an unmodulated optical carrier. This is consistent with theoretical analysis.

To verify the performance of our proposed scheme at low frequency, we set the carrier frequencies of two microwave vector signals to 1 GHz. The measured spectra and corresponding EVMs of recovered two vector signals in the case of BTB and 25-km SMF transmission are given in Fig. 3. Fig. 3(a) and Fig. 3(c) show measured electrical spectra of 100-Msymbol/s QPSK vector signal in the case of BTB and 25-km SMF transmission respectively, where we can see two electrical spectra are pure. The corresponding constellation diagrams are depicted in Fig. 3(b) and Fig. 3(d). The measured EVMs are respectively 3.32% and 4.78%. Measured electrical spectra of 50-Msymbol/s 16-QAM vector signal in the case of BTB and 25-km SMF transmission are respectively given in Fig. 3(e) and Fig. 3(g), in which no interference signals are observed in the electrical spectra. The corresponding constellation diagrams are respectively denoted in Fig. 3(f) and Fig. 3(h). The measured EVMs are respectively 3.97% and 5.44%. Compared with [13], these experimental results indicate that our proposed link working at low frequency has better transmission performance.

To verify the performance of the scheme at different frequencies, then we change the carrier frequency of I(t) and Q(t) to 6 GHz. In the case of BTB and 25-km SMF transmission, by adjusting the PC, I(t) and Q(t) are successfully demodulated after photo-detection by BPD. We measured the performance of this link in terms of EVM. The measured spectra and corresponding EVMs of demodulated two signals in the case of BTB and 25-km SMF transmission are given in Fig. 4. In the case of BTB, it can be seen from Fig. 4(a) and Fig. 4(e) that measured electrical spectra of 100-Msymbol/s QPSK signal and 50-Msymbol/s 16-QAM signal are spurious-free. The corresponding constellation diagrams of two signals are depicted in Fig. 4(b) and Fig. 4(f). The EVM of QPSK signal is 3.41% and the EVM of 16-QAM signal is 4.89%, which indicate that they have been successfully demodulated. After 25-km SMF transmission, measured electrical spectra of two vector signals are depicted in Fig. 4(c) and Fig. 4(g), which can be clearly seen that their electrical spectra are pure. The corresponding constellation diagrams are respectively provided in Fig. 4(d) and Fig. 4(h). The measured EVMs are respectively 5.34% and 5.51%. The measured results show that our proposed structure has good transmission capability. Compared Fig. 3 and Fig. 4, we can see that the transmission performance of the system is similar at different frequencies.

Subsequently, we measured EVMs and calculated BERs of I(t) and Q(t) versus received optical power in the case of BTB and 25-km SMF transmission. We can see from Fig. 5 that EVMs and BERs for BTB and 25-km SMF transmission are similar, indicating that the system has good transmission performance. As shown in Fig. 5(a), when we change the received optical power from -22.5 dBm to -5.5 dBm with 1dBm step, EVMs gradually decrease. This is because the performance of EVMs can be improved with the increase of SNR [16]. As given in Fig. 5(b), when the received optical power is greater than -20 dBm, the corresponding BERs are less than $3\times10e\text{-}3$. Therefore, we can utilize forward error correction (FEC) technique to carry out error-free transmission in proposed link [17]. According to equation (1) in [16], the EVM is only associated with SNR. Therefore, the EVM relative to the received optical power curve of QPSK signal is similar to that of 16-QAM signal. Based on the equations (19) and (20) shown in [8], the corresponding BERs are calculated by MATLAB. With the decrease of EVM, the BER of QPSK signal changes greatly, while the BER of 16QAM signal changes more smoothly. Fig. 5(c) shows that when the

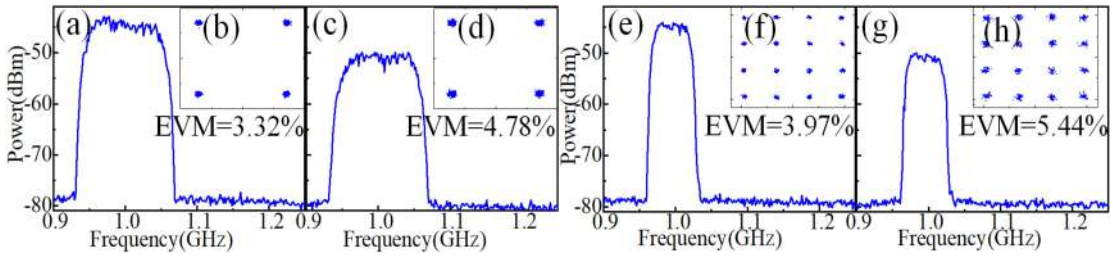

Fig. 3. (a) Measured spectrum and (b) EVM of 100-Msymbol/s QPSK vector signal with 1 GHz carrier frequency in the case of BTB. (c) Measured spectrum and (d) EVM of 100-Msymbol/s QPSK vector signal with 1 GHz carrier frequency after 25-km SMF transmission. (e) Measured spectrum and (f) EVM of 50-Msymbol/s 16-QAM vector signal with 1 GHz carrier frequency in the case of BTB. (g) Measured spectrum and (h) EVM of 50-Msymbol/s 16-QAM vector signal with 1 GHz carrier frequency after 25-km SMF transmission.

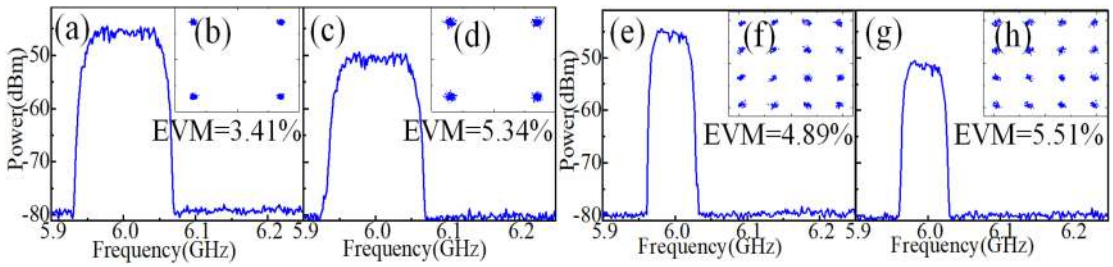

Fig. 4. (a) Measured spectrum and (b) EVM of 100-Msymbol/s QPSK vector signal with 6 GHz carrier frequency in the case of BTB. (c) Measured spectrum and (d) EVM of 100-Msymbol/s QPSK vector signal with 6 GHz carrier frequency after 25-km SMF transmission. (e) Measured spectrum and (f) EVM of 50-Msymbol/s 16-QAM vector signal with 6 GHz carrier frequency in the case of BTB. (g) Measured spectrum and (h) EVM of 50-Msymbol/s 16-QAM vector signal with 6 GHz carrier frequency after 25-km SMF transmission.

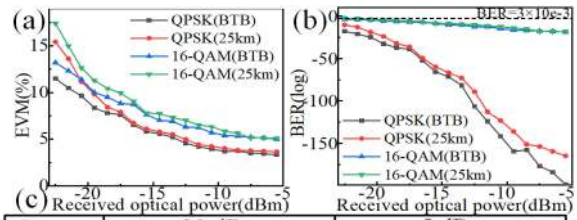

(c)

Power	-20 dBm		-5 dBm	
signal	QPSK	16-QAM	QPSK	16-QAM
BTB	EVM=9.17%	EVM=10.68%	EVM=3.35%	EVM=5.02%
25-km SMF	EVM=10.40%	EVM=11.87%	EVM=3.61%	EVM=5.16%

Fig. 5. (a) Measured EVMs and (b) calculated BERs of QPSK and 16-QAM vector signals versus received optical power in the case of BTB and 25-km SMF transmission. (c) Measured EVMs of QPSK and 16-QAM signals in the case of BTB and 25-km SMF transmission for received optical powers of −20 dBm and −5 dBm.

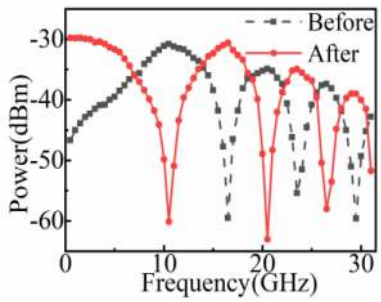

Fig. 6. Measured signal power as a function of the signal frequency for 25-km SMF transmission before the compensation plotted by black dashed line and after the compensation plotted by red solid line.

received optical power is -20 dBm and -5 dBm, measured EVMs of I(t) and Q(t) in the case of BTB and 25-km SMF transmission. We can see that these constellation diagrams are correct and clear. EVMs fluctuate very little after 25-km SMF transmission, which shows that SMF transmission has small effect on link performance.

Our proposed scheme can overcome the chromatic dispersion-induced power fading via adjusting the PC before the PBS [20]. Next, we demonstrate this experimentally. A frequency sweep signal from 0.5 GHz to 31 GHz replaces the vector signal I(t) and the vector signal Q(t) is turned off. After 25-km SMF transmission, measured signal power as a function of signal frequency is plotted by black dashed line in Fig. 6. As can be seen that measured signal power decays periodically as the frequency increases and the fading points are at about 16.5 GHz, 23.5 GHz and 29.5 GHz. After adjusting the PC, the frequency response is plotted by a red solid line in Fig. 6. The fading points are shifted to the peak points, which shows that dispersion-induced power fading can be overcome. With increase of signal frequency, measured signal power gradually decreases. There are three possible reasons: (1) As the frequency increases, the modulation efficiency of modulator becomes worse; (2) The responsivity of

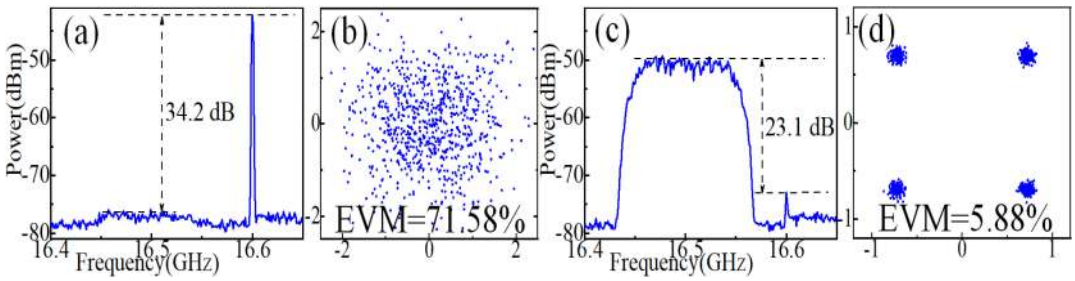

Fig. 7. Measured spectra of QPSK signal with 16.5-GHz carrier frequency and 16.6-GHz single tone before (a) and after (c) compensation of dispersion-induced power fading. Measured EVMs of QPSK signal with 16.5-GHz carrier frequency before (b) and after (d) compensation of dispersion-induced power fading.

TABLE I
PERFORMANCE COMPARISON

Ref.	LO laser source	Power of Signal1	Power of Signal2	Dispersion Compensation	Electric device
This work	None	16QAM (P=-20.5dBm)	QPSK (P=-23.5dBm)	Yes	None
[8]	Needed	16QAM (P=-19dBm)	QPSK (P=-21.5dBm)	No	None
[10]	Needed	16QAM (P=-18dBm)	16QAM (P=-17dBm)	No	180° electric coupler
[12]	None	16QAM (P<-19dBm)	16QAM (P=-11dBm)	No	180° electric coupler
[13]	None	16QAM (P=-2dBm)	QPSK (P=-1.5dBm)	No	None
[15]	None	16QAM (P=-4dBm)	QPSK (P=-1dBm)	Yes	None

BPD becomes lower at a higher frequency; (3) With the increase of signal frequency, the insertion loss of cable increases.

Subsequently, we verify the ability of the link to compensate power fading for vector signal. Limited by the vector signal generator (R&S SMBV100A, 19 KHz-6 GHz), another signal generator (Agilent 83630B) is used to generate a 16.6-GHz single tone as Q(t). We set the vector signal I(t) as a 100-Msymbol/s QPSK signal with a carrier frequency of 16.5 GHz. Measured electrical spectra and EVMs before and after compensation of power fading are shown in Fig. 7. As shown in Fig. 7(a) and Fig. 7(b), affected by dispersion-induced power fading, the QPSK signal is almost submerged by noise and the ratio of the single-tone signal to QPSK signal is 34.2 dB. Therefore, the QPSK signal cannot be demodulated correctly before compensation of power fading and its constellation diagram is chaotic with an EVM of 71.58%. After adjusting the PC, dispersion-induced power fading is overcome and the corresponding electrical spectra and constellation diagram are depicted in Fig. 7(c) and Fig. 7(d), respectively. We can see that the ratio of QPSK signal to single-tone signal is 23.1 dB and the constellation diagram is clear and orderly with an EVM of 5.88%, which show that the system has a good ability to overcome chromatic dispersion-induced power fading for vector signal. It should be noted that because fiber-dispersion limits instantaneous bandwidth, ultra-wideband signals will be affected.

Finally, we give the comparison between the proposed link and other links. Compared with traditional RoF links [21]–[24], the proposed link can transmit two vector signals over an optical carrier, so its spectral efficiency is doubled. Compared with double spectral-efficient RoF links shown in Table 1, the performance of our proposed link is relatively good. According to [16], the maximum EVM specifications of QPSK and 16QAM signals are 17.5% and 12.5%, respectively. To compare performance of these links, Table I gives the corresponding received optical power (P) when the EVM of QPSK and 16QAM signals are 17.5% and 12.5%, respectively. It can be seen that our link is dispersion-free and its performance is relatively good. Under the same EVMs, our proposed link has lower optical power demand, which is of significance to actual system. Besides, the proposed system is an all-optical link without filters and electrical components, so it has a wide operating frequency range.

IV. CONCLUSION

We propose and experimentally demonstrate an all-optical RoF link with simultaneous double spectral-efficient transmission and compensation of chromatic dispersion-induced power fading. Experimental results show that a single optical carrier can transmit 100-Msymbol/s QPSK signal and 50-Msymbol/s 16-QAM signal simultaneously. Compared with the traditional RoF link, the spectral efficiency is doubled. In the case of 25-km SMF transmission, the EVM of QPSK signal with 6 GHz carrier frequency is 5.34% and the EVM of 16-QAM signal with 6 GHz carrier frequency is 5.51%, which show that the system

has good transmission performance. The EVM of QPSK signal with 16.5-GHz carrier frequency after overcoming chromatic dispersion-induced power fading is 5.88%, which shows that the link can overcome dispersion-induced power fading. The proposed system is an all-optical link without electrical components, so it has a wide working frequency range. Our proposed link can be applied in wireless access networks, optical fronthaul link for 5G and MIMO systems.

REFERENCES

[1] J. Capmany and D. Novak, "Microwave photonics combines two worlds," *Nature Photon.*, vol. 1, no. 6, pp. 319–330, Jun. 2007.

[2] C. Lim, Y. Tian, C. Ranaweera, T. A. Nirmalathas, E. Wong, and K.-L. Lee, "Evolution of radio-over-fiber technology," *J. Lightw. Technol.*, vol. 37, no. 6, pp. 1647–1656, Mar. 2019.

[3] Y. Zhang *et al.*, "Photonic DPASK/QAM signal generation at microwave/millimeter-wave band based on an electro-optic phase modulator," *Opt. Lett.*, vol. 33, no. 20, pp. 2332–2334, Oct. 2008.

[4] Y. Chi, Y. Li, H. Wang, P. Peng, H. Lu, and G. Lin, "Optical 16QAM-52-OFDM transmission at 4 Gbit/s by directly modulating a coherently injection-locked colorless laser diode," *Opt. Exp.*, vol. 20, no. 18, pp. 20071–20077, Aug. 2012.

[5] P.-T. Shih, C.-T. Lin, W.-J. Jiang, Y.-H. Chen, J. (J.) Chen, and S. Chi, "Full duplex 60-GHz RoF link employing tandem single sideband modulation scheme and high spectral efficiency modulation format," *Opt. Exp.*, vol. 17, no. 22, pp. 19501–19508, Oct. 2009.

[6] A. Kanno *et al.*, "All-spectrum fiber-wireless transmission for 5G backhaul and fronthaul links," in *Proc. Opt. Fiber Commun. Conf.*, Anaheim, CA, USA, 2016, Art. no. Th2A.26.

[7] R. Q. Shaddad, A. B. Mohammad, and A. M., "Al-hetar, Spectral efficient hybrid wireless optical broadband access network (WOBAN) based on transmission of wireless MIMO OFDM signals over WDM PON," *Opt. Commun.*, vol. 285, no. 20, pp. 4059–4067, Jun. 2012.

[8] X. Chen and J. Yao, "A high spectral efficiency coherent microwave photonic link employing both amplitude and phase modulation with digital phase noise cancellation," *J. Lightw. Technol.*, vol. 33, no. 14, pp. 3091–3097, Jul. 2015.

[9] X. Chen and J. Yao, "4 × 4 Multiple-input multiple-output coherent microwave photonic link with optical independent sideband and optical orthogonal modulation," *Chin. Opt. Lett.*, vol. 15, no. 1, pp. 1–7, Jan. 2017.

[10] H. Zhang, A. Wen, W. Zhang, W. Zhang, W. Zhai, and Z. Tu, "A novel spectral-efficient coherent radio-over-fiber link with linear digital-phase demodulation," *IEEE Photon. J.*, vol. 12, no. 1, Feb. 2020, Art. no. 5500208.

[11] T. R. Clark, S. R. O'Connor, and M. L. Dennis, "A phase-modulation I/Q-demodulation microwave-to-digital photonic link," *IEEE Trans. Microw. Theory Techn.*, vol. 58, no. 11, pp. 3039–3058, Nov. 2010.

[12] H. Zhang, A. Wen, W. Zhang, W. Zhang, and Z. Tu, "A spectral-efficient self-homodyne-detected microwave photonic link with an extended fiber-reach," *IEEE Photon. Technol. Lett.*, vol. 30, no. 19, pp. 1719–1722, Oct. 2018.

[13] Y. Han, W. Zhang, J. Zhang, and J. P. Yao, "Two microwave vector signal transmission on a single optical carrier based on PM-IM conversion using an on-chip optical Hilbert transformer," *J. Lightw. Technol.*, vol. 36, no. 3, pp. 682–688, Feb. 2018.

[14] U. Gliese, S. Norskov, and T. N. Nielsen, "Chromatic dispersion in fiber-optic microwave and millimeter-wave links," *IEEE Trans. Microw. Theory Techn.*, vol. 44, no. 10, pp. 1716–1724, Oct. 1996.

[15] W. Zhang, A. Wen, Y. Li, and J. Ma, "A high spectral efficiency microwave photonic link with optimization of chromatic-dispersion-induced power fading," *J. Lightw. Technol.*, vol. 37, no. 4, pp. 1123–1132, Feb. 2019.

[16] H. S. Chung, S. H. Cho, C. G. Han, S. Lee, J. C. Lee, and J. H. Lee, "Design of RoF based mobile fronthaul link with multi-IF carrier for LTE/LTE-A signal transmission," in *Proc. IEEE Int. Topics Meeting Microw. Photon.*, 2014, Art. no. 303-306.

[17] R. Schmogrow *et al.*, "512QAM Nyquist sinc-pulse transmission at 54 Gbit/s in an optical bandwidth of 3 GHz," *Opt. Exp.*, vol. 20, no. 6, pp. 6439–6447, Mar. 2012.

[18] W. Li, W. T. Wang, and N. H. Zhu, "Broadband microwave photonic splitter with arbitrary amplitude ratio and phase shift," *IEEE Photon. J.*, vol. 6, no. 6, Dec. 2014, Art. no. 5501507.

[19] [Online]. Available: https://www.generalphotonics.com/index.php/product/pos-002-polarizationtracker/

[20] W. Zhai, A. Wen, W. Zhang, Z. Tu, H. Zhang, and Z. Xiu, "A multichannel phase tunable microwave photonic mixer with high conversion gain and elimination of dispersion-induced power fading," *IEEE Photon. J.*, vol. 10, no. 1, Feb. 2018, Art. no. 5500210.

[21] S. Li, X. Zheng, H. Zhang, and B. Zhou, "Compensation of dispersion induced power fading for highly linear radio-over-fiber link using carrier phase-shifted double sideband modulation," *Opt. Lett.*, vol. 36, no. 4, pp. 546–548, Feb. 2011.

[22] J. Liu, X. Wu, C. Huang, H. K. Tsang, and C. Shu, "Compensation of dispersion-induced power fading in analog photonic links by gain-transparent SBS," *IEEE Photon. Technol. Lett.*, vol. 30, no. 8, pp. 688–691, Apr. 2018.

[23] Y. Cui *et al.*, "Overcoming chromatic-dispersion-induced power fading in ROF links employing parallel modulators," *IEEE Photon. Technol. Lett.*, vol. 24, no. 14, pp. 1173–1175, Jul. 2012.

[24] J. Niu *et al.*, "Mitigation of dispersion-induced power fading in long-haul analog optical link based on 2-Ch phase modulator," in *Proc. IEEE Opt. Fiber Commun. Conf. Expo.*, JW2A.76, pp. 1–3, 2012.